Quasi-linear heating and acceleration in bi-Maxwellian plasmas

Petr Hellinger,[1] Thierry Passot,[2] Pierre-Louis Sulem,[2] and Pavel M. Trávníček[3,1]
[1)] *Astronomical Institute & Institute of Atmospheric Physics, AS CR Bocni II/1401, CZ-14131 Prague, Czech Republic*
[2)] *Université de Nice Sophia Antipolis, CNRS, Observatoire de la Côte d'Azur, BP 4229, 06304 Nice Cedex 4, France*
[3)] *Space Sciences Laboratory, University of Berkeley, 7 Gauss Way, Berkeley, CA 94720, U.S.A.*

(Dated: 12 June 2014)

Quasi-linear acceleration and heating rates are derived for drifting bi-Maxwellian distribution functions in a general nonrelativistic case for arbitrary wave vectors, propagation angles, and growth/damping rates. The heating rates in a proton-electron plasma due to ion-cyclotron/kinetic Alfvén and mirror waves for a wide range of wavelengths, directions of propagation and growth or damping rates are explicitly computed.

PACS numbers: ?

I. INTRODUCTION

Heating properties of low-amplitude electromagnetic waves can be estimated by considering the linear expressions of the particle current $\boldsymbol{j}_\mathrm{s}$ and of the electric field $\boldsymbol{E}$, and calculating the product $\boldsymbol{j}_\mathrm{s}\cdot\boldsymbol{E}$ (for symbol definitions see Appendix).[1] This approach is compatible with the quasi-linear approximation which may, to some extent, describe the nonlinear properties of small-amplitude electromagnetic waves in collisionless plasmas. This approximation assumes a superposition of incoherent linear modes which at the second order (in the wave amplitude) affect the background averaged particle distribution functions.[2–4]

Calculation of quasi-linear predictions is generally delicate. Some information of the quasi-linear expectations for instabilities may be obtained by applying the quasi-linear diffusion operator on the initial particle velocity distribution function.[5,6] To make the calculation tractable, one may consider a prescribed velocity distribution function (typically, a bi-Maxwellian). Such an approach has been used to investigate the heating properties of unstable modes in special cases (unmagnetized plasmas, parallel or strongly oblique propagation with respect to the ambient magnetic field, a long-wavelength or low-frequency limit, ...).[7–10] For damped waves these results have been analytically continued by taking the limit $\gamma\to 0+$.[11,12] However, this limit is only applicable for weakly damped modes ($\gamma\ll\omega_r$). Moreover, the momentum and energy exchanges between particles and waves cease[13] and the quasi-linear diffusion is then likely reduced. General expression for parallel and perpendicular heating rates in the case of (non-drifting) bi-Maxwellian has been derived by Ref. 14 but implemented only for unstable modes. In this paper, we apply the quasi-linear diffusion operator on a drifting bi-Maxwellian velocity distribution function and calculate the moments, the acceleration and the heating rates for electromagnetic waves in a general nonrelativistic case for arbitrary wave vectors, propagation angles, and growth/damping rates. The paper is organized as follows: Section II summarizes the quasi-linear approximation. In Section III we derive the acceleration and heating rates in the case of bi-Maxwellian distribution functions. In Section IV we investigate, as examples, the heating properties of both stable and unstable Alfvén ion cyclotron/kinetic and mirror waves. Obtained results are summarized in Section V.

II. QUASI-LINEAR THEORY

The quasi-linear theory assumes a superposition of noninteracting random-phase linear waves with wave vectors $\boldsymbol{k}$ and (complex) frequencies ω, together with a fluctuating electric field $\delta\boldsymbol{E}$, which fulfill the linear conditions

$$\det\mathbf{D}(\boldsymbol{k},\omega)=0 \quad\text{and}\quad \mathbf{D}(\boldsymbol{k},\omega)\cdot\delta\boldsymbol{E}(\boldsymbol{k},\omega)=0, \qquad (1)$$

where the dispersion tensor $\mathbf{D}$ is expressed in terms of the average particle velocity distribution function f_s as

$$\mathbf{D}=\left(1-\frac{k^2c^2}{\omega^2}-\sum_\mathrm{s}\frac{\omega_{ps}^2}{\omega^2}\right)\mathbf{1}+\frac{\boldsymbol{k}\boldsymbol{k}c^2}{\omega^2} -\sum_\mathrm{s}\frac{\omega_{ps}^2}{\omega^2}\sum_{n=-\infty}^{\infty}\int\frac{k_\parallel\frac{\partial f_\mathrm{s}}{\partial v_\parallel}+n\frac{\omega_\mathrm{cs}}{v_\perp}\frac{\partial f_\mathrm{s}}{\partial v_\perp}}{k_\parallel v_\parallel-\omega+n\omega_\mathrm{cs}}\overline{\boldsymbol{w}_{sn}}\boldsymbol{w}_{sn}\mathrm{d}^3v, \qquad (2)$$

with

$$\boldsymbol{w}_{sn}=\left(nJ_n\frac{\omega_\mathrm{cs}}{k_\perp},iJ_n'v_\perp,J_nv_\parallel\right). \qquad (3)$$

The second order effect of the wave modes on the particle distribution functions leads to the diffusion equation

$$\frac{\partial f_\mathrm{s}}{\partial t}=\frac{\partial}{\partial v_\parallel}\left(\mathcal{D}_{\parallel\parallel\mathrm{s}}\frac{\partial f_\mathrm{s}}{\partial v_\parallel}+\mathcal{D}_{\parallel\perp\mathrm{s}}\frac{\partial f_\mathrm{s}}{\partial v_\perp}\right) +\frac{1}{v_\perp}\frac{\partial}{\partial v_\perp}v_\perp\left(\mathcal{D}_{\perp\parallel\mathrm{s}}\frac{\partial f_\mathrm{s}}{\partial v_\parallel}+\mathcal{D}_{\perp\perp\mathrm{s}}\frac{\partial f_\mathrm{s}}{\partial v_\perp}\right), \qquad (4)$$

where the diffusion tensor $\boldsymbol{\mathcal{D}}$ may be given in the following explicit form[4,6]

$$\mathcal{D}_{IJ\mathrm{s}}=\frac{q_\mathrm{s}^2}{m_\mathrm{s}^2}\sum_\mathrm{modes}\Im\sum_{n=-\infty}^{\infty}\frac{\overline{(\delta\boldsymbol{E}\cdot\boldsymbol{a}_{Isn})}(\boldsymbol{a}_{Jsn}\cdot\delta\boldsymbol{E})}{k_\parallel v_\parallel+n\omega_\mathrm{cs}-\omega}, \qquad (5)$$

with $I, J = \parallel, \perp$. In the frame where $\boldsymbol{k} = (k_\perp, 0, k_\parallel)$ the vectors $\boldsymbol{a}_{\parallel sn}$ and $\boldsymbol{a}_{\parallel sn}$ are given by

$$\boldsymbol{a}_{\parallel sn} = \left(\frac{n\omega_{cs} k_\parallel}{\omega k_\perp} J_n, i J_n' \frac{k_\parallel v_\perp}{\omega}, \frac{\omega - n\omega_{cs}}{\omega} J_n \right)$$
$$\boldsymbol{a}_{\perp sn} = \left(\frac{\omega - k_\parallel v_\parallel}{\omega} \frac{n\omega_{cs}}{k_\perp v_\perp} J_n, i \frac{\omega - k_\parallel v_\parallel}{\omega} J_n', \frac{n\omega_{cs} v_\parallel}{\omega v_\perp} J_n \right).$$

The above expressions are only valid for unstable modes with $\gamma > 0$; for $\gamma \leq 0$ they must be analytically continued.[13]

III. ACCELERATION AND HEATING RATES

For drifting bi-Maxwellian velocity distribution functions

$$f_{\rm s}^{\rm BM} = \frac{1}{(2\pi)^{3/2} v_{\rm s\parallel} v_{\rm s\perp}^2} e^{-\frac{v_\perp^2}{2v_{\rm s\perp}^2} - \frac{(v_\parallel - v_{\rm s0})^2}{2v_{\rm s\parallel}^2}}, \tag{6}$$

the dispersion matrix $\mathbf{D}$ is given by[15]

$$\mathbf{D} = \left(1 - \frac{k^2 c^2}{\omega^2}\right) \mathbf{1} + \frac{\boldsymbol{k}\boldsymbol{k} c^2}{\omega^2} + \sum_{\rm s} \frac{\omega_{ps}^2}{\omega^2} \mathbf{Q}_{\rm s}, \tag{7}$$

where

$$\mathbf{Q}_{\rm s} = \begin{pmatrix} A_{\rm s} - 1 & 0 & (1 - A_{\rm s}) \frac{k_\perp}{k_\parallel} \\ 0 & A_{\rm s} - 1 & 0 \\ (1 - A_{\rm s}) \frac{k_\perp}{k_\parallel} & 0 & \frac{\omega^2}{k_\parallel^2 v_{\rm s\parallel}^2} + (A_{\rm s} - 1) \frac{k_\perp^2}{k_\parallel^2} \end{pmatrix} \tag{8}$$
$$+ A_{\rm s} \sum_{n=-\infty}^{\infty} \begin{pmatrix} \frac{n^2 \Lambda_n}{\lambda_{\rm s}^2} & i n \Lambda_n' & \frac{n \Lambda_n \eta_{sn}}{\lambda_{\rm s}} \\ -i n \Lambda_n' & \frac{n^2 \Lambda_n}{\lambda_{\rm s}^2} - 2\lambda_{\rm s}^2 \Lambda_n' & -i \lambda_{\rm s} \Lambda_n' \eta_{sn} \\ \frac{n \Lambda_n \eta_{sn}}{\lambda_{\rm s}} & i \lambda_{\rm s} \Lambda_n' \eta_{sn} & \Lambda_n \eta_{sn}^2 \end{pmatrix} \Xi_{sn},$$

and $A_{\rm s} = v_{\rm s\perp}^2 / v_{\rm s\parallel}^2$, $\lambda_{\rm s} = k_\perp v_{\rm s\perp} / \omega_{cs}$, $\Xi_{sn} = \xi_{sn} Z(\zeta_{sn})$,

$$\eta_{sn} = \frac{\omega - n\omega_{cs}}{k_\parallel v_{\rm s\perp}}, \quad \zeta_{sn} = \frac{\omega - k_\parallel v_{\rm s0} - n\omega_{cs}}{\sqrt{2} k_\parallel v_{\rm s\parallel}},$$
$$\xi_{sn} = \frac{\omega - k_\parallel v_{\rm s0} - (1 - 1/A_{\rm s}) n\omega_{cs}}{\sqrt{2} k_\parallel v_{\rm s\parallel}}.$$

Here, $\Lambda_n = \Lambda_n(\lambda_{\rm s}^2)$ are the exponentially scaled modified Bessel functions of the first kind (Λ_n' being its derivative) and $Z = Z(\zeta_{sn})$ is the plasma dispersion function.

For the initial change of the parallel particle momentum starting from the bi-Maxwellian velocity distribution function,

$$\frac{\partial p_{\rm s\parallel}}{\partial t} = m_{\rm s} n_{\rm s} \int \frac{\partial f_{\rm s}}{\partial t} v_\parallel {\rm d}^3 v \tag{9}$$

where $\partial f_{\rm s} / \partial t$ is replaced by $\partial / \partial \boldsymbol{v} \cdot \boldsymbol{\mathcal{D}} \cdot \partial f_{\rm s}^{\rm BM} / \partial \boldsymbol{v}$. We thus get

$$\frac{\partial p_{\rm s\parallel}}{\partial t} = \epsilon_0 \frac{\omega_{ps}^2}{|\omega|^2} k_\parallel A_{\rm s} \sum_{n=-\infty}^{\infty} \mathcal{H}_{sn} \Im \Xi_{sn}, \tag{10}$$

where

$$\mathcal{H}_{sn} = \Lambda_n \left| \frac{n}{\lambda_{\rm s}} \delta E_x + \eta_{sn} \delta E_z \right|^2 + \left(\frac{n^2 \Lambda_n}{\lambda_{\rm s}^2} - 2\lambda_{\rm s}^2 \Lambda_n' \right) |\delta E_y|^2 + \lambda_{\rm s} \Lambda_n' 2 \Im \overline{\delta E_y} \left(\frac{n}{\lambda_{\rm s}} \delta E_x + \eta_{sn} \delta E_z \right). \tag{11}$$

Hereafter we drop the sum over the modes, as we are interested in the contribution of a given mode to the quasi-linear transport coefficients. Note that the analytic continuation is hidden in the plasma dispersion function.

Similarly for the particle parallel kinetic energy $\mathcal{E}_{\rm s\parallel} = m_{\rm s} n_{\rm s} \int f_{\rm s} v_\parallel^2 {\rm d}^3 v / 2$, we get the heating rate (per mode)

$$\frac{\partial \mathcal{E}_{\rm s\parallel}}{\partial t} = \epsilon_0 \frac{\omega_{ps}^2}{|\omega|^2} \gamma A_{\rm s} \left(\left| \delta E_x - \frac{k_\perp}{k_\parallel} \delta E_z \right|^2 + |\delta E_y|^2 \right) + \epsilon_0 \frac{\omega_{ps}^2}{k_\parallel^2 v_{\rm s\parallel}^2} \gamma |\delta E_z|^2 + \epsilon_0 \frac{\omega_{ps}^2}{|\omega|^2} A_{\rm s} \sum_{n=-\infty}^{\infty} \mathcal{H}_{sn} \Im(\omega - n\omega_{cs}) \Xi_{sn}, \tag{12}$$

whereas for the particle perpendicular kinetic energy $\mathcal{E}_{\rm s\perp} = m_{\rm s} n_{\rm s} \int f_{\rm s} v_\perp^2 {\rm d}^3 v / 2$ the heating rate (per mode) is

$$\frac{\partial \mathcal{E}_{\rm s\perp}}{\partial t} = \epsilon_0 \frac{\omega_{ps}^2}{|\omega|^2} \gamma (1 - 2A_{\rm s}) \left(\left| \delta E_x - \frac{k_\perp}{k_\parallel} \delta E_z \right|^2 + |\delta E_y|^2 \right) + 2\epsilon_0 \frac{\omega_{ps}^2}{|\omega|^2} A_{\rm s} \sum_{n=-\infty}^{\infty} \Re \frac{\gamma \overline{\omega}}{k_\parallel v_{\rm s\perp}} \overline{\delta E_z} \times \left[\Lambda_n \left(\frac{n}{\lambda_{\rm s}} \delta E_x + \eta_{sn} \delta E_z \right) + i \lambda_{\rm s} \Lambda_n' \delta E_y \right] \Xi_{sn} + \epsilon_0 \frac{\omega_{ps}^2}{|\omega|^2} A_{\rm s} \sum_{n=-\infty}^{\infty} \mathcal{H}_{sn} \Im \left(n\omega_{cs} - 2i\gamma \right) \Xi_{sn}. \tag{13}$$

One can easily verify (using (1)) that these expressions conserve the total parallel momentum and the energy as in the original problem.[13]

The resulting total heating rates, $\partial \mathcal{E}_{\rm s} / \partial t = \partial \mathcal{E}_{\rm s\parallel} / \partial t + \partial \mathcal{E}_{\rm s\perp} / \partial t$ are equivalent to those obtained from the linear $\boldsymbol{j}_{\rm s} \cdot \boldsymbol{E}$ approach.[1] Setting the drift velocities zero, one finds the heating rates of Ref. 14 and, in the limit $\gamma \to 0$, one recovers the previous results of Ref. 12, as well as when concentrating to the parallel limit ($k_\perp \to 0$) for which one gets[9]

$$\frac{\partial p_{\rm s\parallel}}{\partial t} = \epsilon_0 \frac{\omega_{ps}^2}{k_\parallel v_{s\parallel}^2} |\delta E_z|^2 \Im \Xi_{\rm s0} + \epsilon_0 \frac{\omega_{ps}^2}{|\omega|^2} k_\parallel A_{\rm s} \sum_{n=\pm 1} \frac{|\delta E_n|^2}{2} \Im \Xi_{sn}, \tag{14}$$

$$\frac{\partial \mathcal{E}_{s\parallel}}{\partial t} = \epsilon_0 \frac{\omega_{ps}^2}{|\omega|^2}\gamma A_s \left(|\delta E_x|^2 + |\delta E_y|^2\right) + \epsilon_0 \frac{\omega_{ps}^2}{k_\parallel^2 v_{s\parallel}^2}\gamma |\delta E_z|^2 + \epsilon_0 \frac{\omega_{ps}^2}{k_\parallel^2 v_{s\parallel}^2} |\delta E_z|^2 \Im\omega\Xi_{s0} + \epsilon_0 \frac{\omega_{ps}^2}{|\omega|^2} A_s \sum_{n=\pm 1} \frac{|\delta E_n|^2}{2} \Im(\omega - n\omega_{cs})\Xi_{sn}, \quad (15)$$

and

$$\frac{\partial \mathcal{E}_{s\perp}}{\partial t} = \epsilon_0 \frac{\omega_{ps}^2}{|\omega|^2}\gamma(1 - 2A_s) \left(|\delta E_x|^2 + |\delta E_y|^2\right) + \epsilon_0 \frac{\omega_{ps}^2}{|\omega|^2} A_s \sum_{n=\pm 1} \frac{|\delta E_n|^2}{2} \Im\left(n\omega_{cs} - 2i\gamma\right) \Xi_{sn}, \quad (16)$$

where $\delta E_n = \delta E_x + in\delta E_y$.

IV. HEATING BY ION-CYCLOTRON AND MIRROR WAVES

A. Ion-cyclotron waves – isotropic protons

Let us consider Alfvén ion cyclotron/kinetic waves in a plasma consisting of isotropic (i.e. Maxwellian) protons and electrons, with $\omega_{pe}/\omega_{ce} = 100$, $\beta_p = \beta_e = 0.5$. In this case, the ion-cyclotron waves (left-handed at quasi-parallel propagation angles) are stable. Their dispersion relation is shown in Fig. 1 which displays as color scale plots the real frequency (top panel) and the damping rate (bottom panel) as functions of the wave vector k and the angle of propagation θ_{kB}.

Using (12) and (13), we get the proton heating/cooling rates for the bi-Maxwellian velocity distribution function. These rates (per mode) are shown in Fig. 2 which displays $\partial\mathcal{E}_{p\parallel}/\partial t$ (top panel), $\partial\mathcal{E}_{p\perp}/\partial t$ (middle panel) and $\partial\mathcal{E}_p/\partial t$ (bottom panel) as functions of the wave vector k and the angle of propagation θ_{kB}, as color scale plots. The heating rates are given in units of $\mathcal{E}_{em}\omega_{cp}$, where $\mathcal{E}_{em} = \epsilon_0|\delta\boldsymbol{E}|^2/2 + |\delta\boldsymbol{B}|^2/(2\mu_0)$ is the electromagnetic energy of the given mode.

We see that, in quasiparallel directions, the ion-cyclotron waves heat the protons in the perpendicular direction (an observation consistent with previous results[12]) and cool them in the parallel one for sufficiently short wavelengths (through the cyclotron resonance). At oblique angles, longer wavelength waves heat the protons in the parallel direction and cool them in the perpendicular one (in this case through the Landau resonance[16]). In total, the damped ion cyclotron waves heat protons.

We similarly get the electron heating rates (per mode). Figure 3 shows $\partial\mathcal{E}_{e\parallel}/\partial t$ (top), $\partial\mathcal{E}_{e\perp}/\partial t$ (middle) and $\partial\mathcal{E}_e/\partial t$ (bottom) as functions of the wave vector k and the angle of propagation θ_{kB} as color scale plots. It is seen that the ion cyclotron waves interact weakly with the electrons (for the given range of wave vectors). They cool them in the perpendicular direction and mainly heat them in the parallel direction (except at oblique angles and short wavelengths). In total, electrons are cooled at quasiparallel angles and heated at more oblique angles.

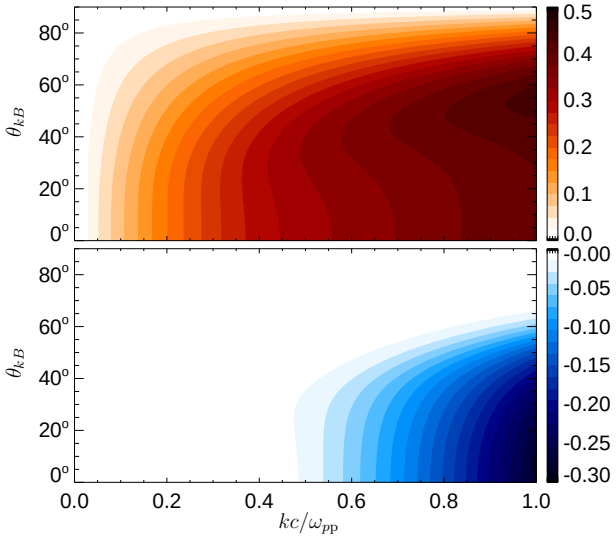

FIG. 1. Dispersion of ion-cyclotron waves (stable case): Color scale plots of (top) the real frequency and (bottom) the growth/damping rate as functions of the wave vector k and the angle of propagation θ_{kB}. The corresponding color scales are shown at right (red shades indicate positive values, and blue shades hold for negative ones). The dotted lines indicate the zero level. Plasma parameters are given in the text.

One can use the energy conservation by the heating processes as a measure of the accuracy of the quasi-linear calculations (and of the result of the linear solver). The heating rates in Figs. 2 and 3 indeed conserve the energy with a precision of $10^{-7}\mathcal{E}_{em}\omega_{cp}$.

B. Ion-cyclotron waves – anisotropic protons

For comparison let us consider a regime where bi-Maxwellian anisotropic protons destabilize the ion-cyclotron waves,[9,17] assuming isotropic electrons with $\omega_{pe}/\omega_{ce} = 100$, $\beta_{p\parallel} = \beta_e = 0.5$, and $A_p = 1.85$. Their dispersion is shown in Fig. 4 which displays the real frequency (top panel) and the growth/damping rate (bottom) as functions of the wave vector k and the angle of propagation θ_{kB} as color scale plots. We observe that the ion cyclotron waves are indeed destabilized around the parallel propagation, the most unstable mode being at parallel propagation with $k_{max} \sim 0.5\omega_{pp}/c$ and a growth rate $\gamma_{max} \sim 10^{-2}\omega_{cp}$. Compared to the isotropic case, the real frequencies are higher and damping rates lower in the presence of temperature anisotropy.

The proton heating rates (per mode) $\partial\mathcal{E}_{p\parallel}/\partial t$ (top), $\partial\mathcal{E}_{p\perp}/\partial t$ (middle) and $\partial\mathcal{E}_p/\partial t$ (bottom) are shown in Fig. 5. In the unstable regime, the ion cyclotron waves heat the protons in the parallel direction and cool in the perpendicular direction; the instability reduces the

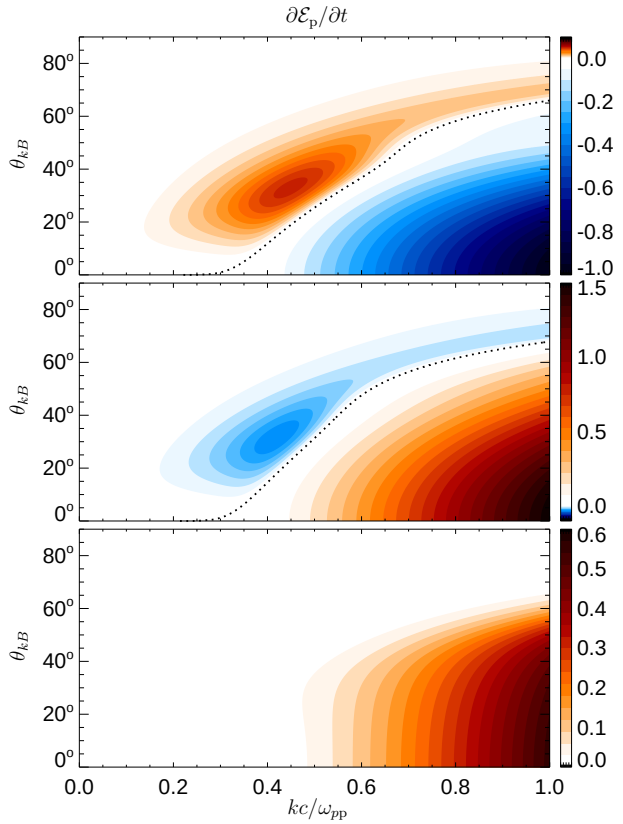

FIG. 2. Proton heating rates for stable ion-cyclotron Alfvén waves: Color scale plots of the parallel (top), perpendicular (middle) and total (bottom) heating rates as functions of the wave vector k and the angle of propagation θ_{kB}. The corresponding color scales are shown at right (red shades indicate positive values, and blue shades negative ones). The dotted lines indicate the zero level. Plasma parameters are given in the text.

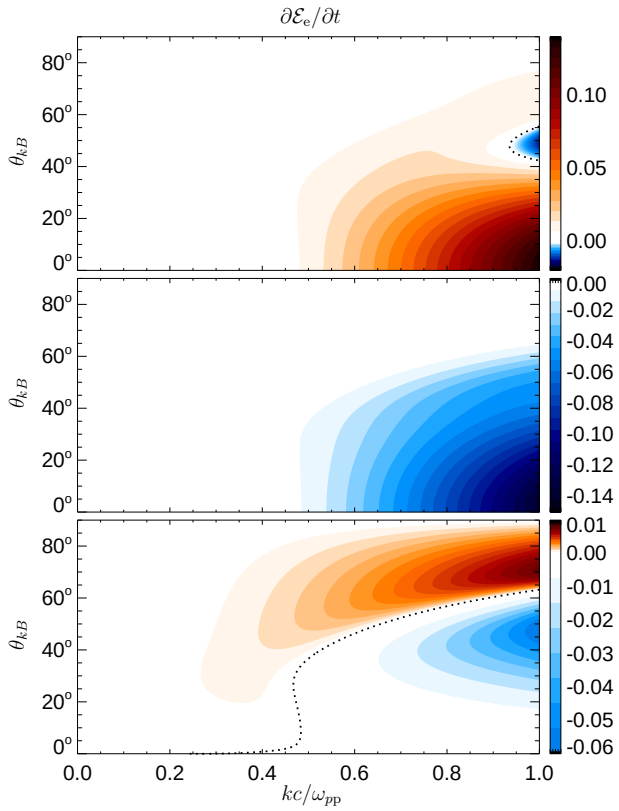

FIG. 3. Same as Fig. 2 for the parallel (top), perpendicular (middle) and total (bottom) electron heating rates for ion-cyclotron Alfvén waves (stable case).

proton temperature anisotropy, as expected. The region where the protons are cooled in the parallel direction and heated in the perpendicular one extends to oblique angles where a similar behavior is seen in the isotropic case. However, for some parameters, parallel cooling is observed at oblique propagation. At quasi-parallel angles and shorter wavelengths, the damped ion cyclotron waves heat the protons in the perpendicular direction and cool them in the parallel one. In total, protons are cooled in the unstable region as expected, but also weakly at oblique propagation, while heating occurs at small wave length in a large range of angles.

The electron heating rates (per mode) $\partial\mathcal{E}_{\mathrm{e}\parallel}/\partial t$ (top), $\partial\mathcal{E}_{\mathrm{e}\perp}/\partial t$ (middle) and $\partial\mathcal{E}_\mathrm{e}/\partial t$ (bottom) are displayed in Fig. 6. It turns out that the electron parallel and perpendicular heating rates in the anisotropic case are similar to those in the isotropic regime, except in the unstable region where the heating rates change signs. Consequently, the total heating rate is also somewhat modified compared to the isotropic case. In the anisotropic case the conservation properties are somewhat deteriorated but still acceptable, the heating rates in Figs. 5 and 6 preserving energy with a precision of $10^{-5}\mathcal{E}_{em}\omega_{c\mathrm{p}}$.

C. Mirror modes

Finally, let us consider the non-propagating mirror modes[18,19] which may be destabilized by the anisotropic protons through the Landau resonance. Again, we assume isotropic electrons and bi-Maxwellian anisotropic protons with $\omega_{pe}/\omega_{ce} = 100$, $\beta_{\mathrm{p}\parallel} = \beta_\mathrm{e} = 1$, and $A_\mathrm{p} = 2$. The mirror dispersion is shown in Fig. 7 which displays the growth/damping rate (bottom) as a function of the wave vector k and the angle of propagation θ_{kB} as color scale plots. The real frequency of the mirror mode is zero. As expected, the mirror waves are destabilized at strongly oblique angles, the most unstable mode being at $\theta_{kB} \simeq 63.9^\mathrm{o}$, with $k_\mathrm{max} \sim 0.35\omega_{pp}/c$ and a growth rate $\gamma_\mathrm{max} \sim 8 \cdot 10^{-3}\omega_{c\mathrm{p}}$.

The proton heating rates (per mode) due to the mirror mode $\partial\mathcal{E}_{\mathrm{p}\parallel}/\partial t$ (top), $\partial\mathcal{E}_{\mathrm{p}\perp}/\partial t$ (middle) and $\partial\mathcal{E}_\mathrm{p}/\partial t$ (bottom) are shown in Fig. 8. The unstable mirror modes heat the protons in the parallel direction and cool them in the perpendicular direction; the instability reduces the proton temperature anisotropy, as expected, similarly to the case of unstable Alfvén ion-cyclotron waves. The

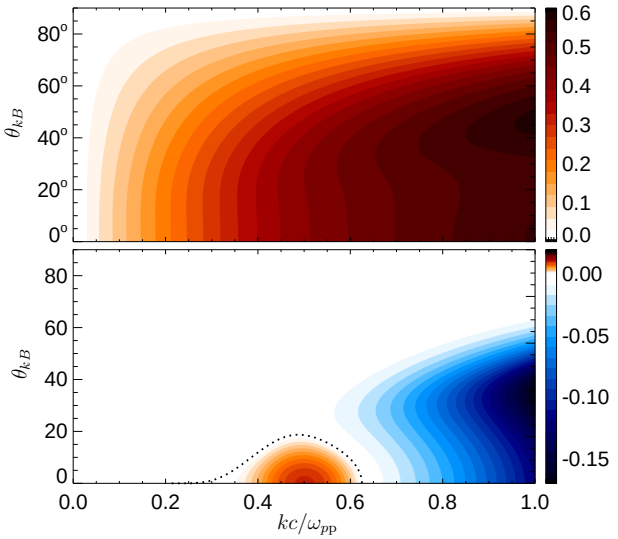

FIG. 4. Dispersion of ion cyclotron waves (unstable case): Color scale plots of the real frequency (top) and growth/damping rate (bottom) as functions of the wave vector k and the angle of propagation θ_{kB}. Plasma parameters are given in the text.

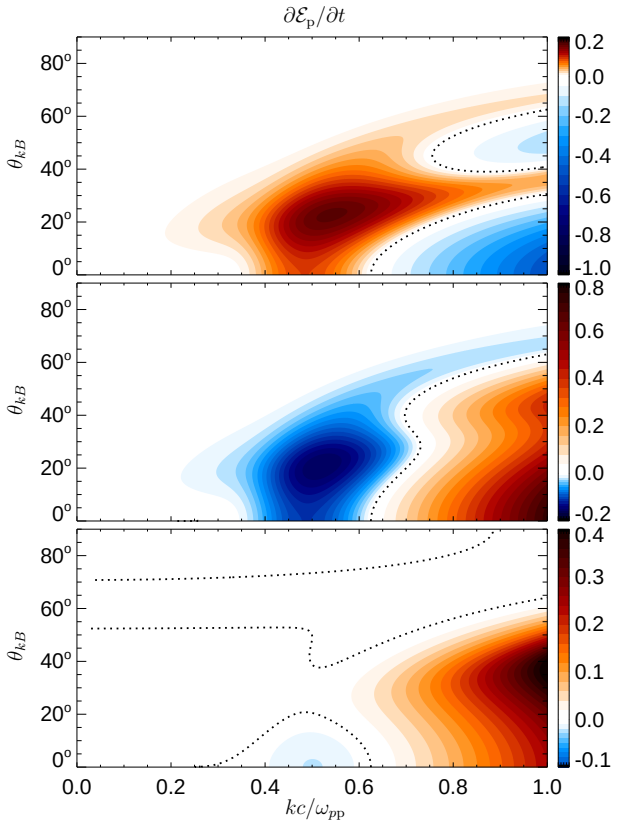

FIG. 5. Same as Fig. 2 for the proton heating rates for ion-cyclotron waves in the unstable regime.

stable/damped mirror modes have the opposite heating properties: they cool the protons in the parallel direction and heat them in the perpendicular direction. In total, protons are cooled in the unstable region and heated in the stable region as expected.

The electron heating rates (per mode) due to the mirror mode $\partial\mathcal{E}_{e\parallel}/\partial t$ (top), $\partial\mathcal{E}_{e\perp}/\partial t$ (middle) and $\partial\mathcal{E}_e/\partial t$ (bottom) are displayed in Fig. 9. The electron heating rates in the parallel and perpendicular directions are qualitatively similar to those of protons. The unstable (stable) mirror modes heat (cool) the electrons in the parallel direction and cool (heat) them in the perpendicular direction. However, in total, electrons are heated in the unstable region and cooled in the stable region. In the mirror case the conservation properties are very good: the heating rates in Figs. 8 and 9 preserve energy with an accuracy of $10^{-7}\mathcal{E}_{em}\omega_{cp}$.

V. DISCUSSION

We computed in this paper the quasi-linear acceleration and heating rates for particle (drifting) bi-Maxwellian velocity distribution functions in a general nonrelativistic case for arbitrary wave vectors, propagation angles, and growth/damping rates, thus extending previous results[9,12,14]. The resulting moment relations form a closed, energy and momentum conserving system that may be used as a fluid closure to kinetic instabilities,[10,14] although the latter are often sensitive to the shape of the velocity distribution function[20] and the assumption that particle velocity distribution functions remain bi-Maxwellian may, in some instances, lead to unphysical results.

The derived expressions (10), (12) and (13) are useful for estimating the acceleration and heating rates of small-amplitude damped waves as well as for analyzing the properties of kinetic instabilities[5] and of the corresponding anomalous transport coefficients.[21] They can also be used to estimate magnetohydrodynamic turbulent heating rates,[22] if the quasi-linear approximation is applicable.

We also presented a full numerical implementation of the theory by considering the heating properties of ion-cyclotron/kinetic Alfvén and mirror waves for a wide range of wavelengths, direction of propagation and growth or damping rates, in proton-electron plasma (using the conservation properties to check the numerical linear and quasi-linear results). The predicted quasi-linear heating is typically anisotropic and often corresponds to a heating in the parallel direction and a cooling in the perpendicular one, or vice versa, with, as in the case of ion-cyclotron waves, heating of one particle species and cooling of the other one. This effect could provide an interpretation of the proton parallel cooling and perpendicular heating observed in the solar wind.[23]

The results presented here are derived on the basis of the quasi-linear theory for random-phase weak-amplitude waves, and the predicted heating or cooling concerns the leading order perturbation of a bi-Maxwellian equilib-

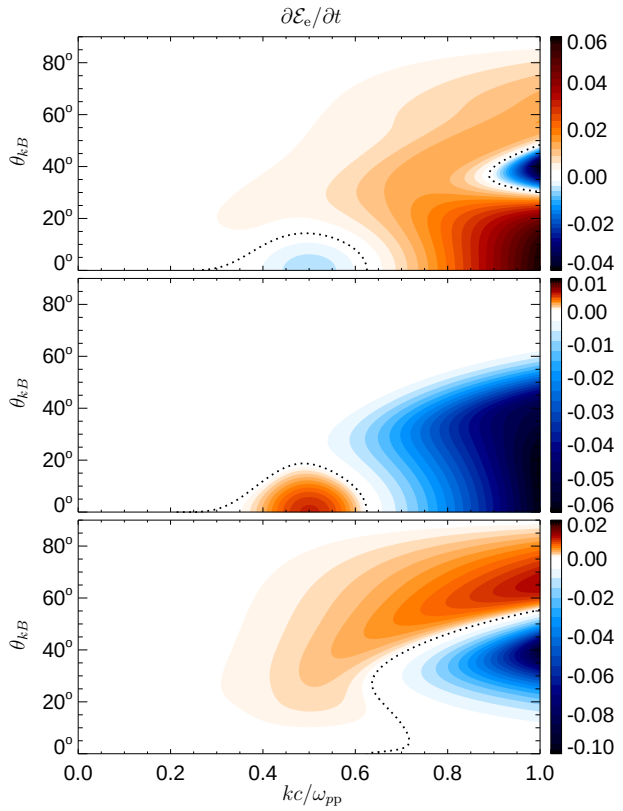

FIG. 6. Same as Fig. 3 for the electron heating rates in the case of ion-cyclotron waves (unstable regime).

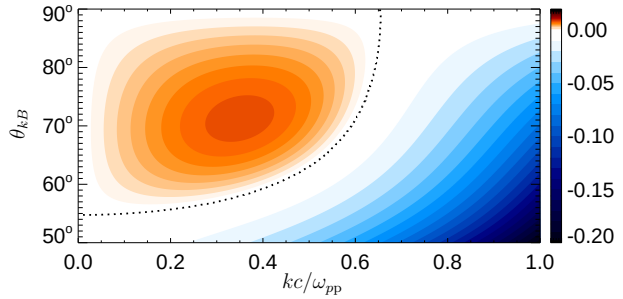

FIG. 7. Dispersion of mirror waves: Color scale plot of the growth/damping rate as functions of the wave vector k and the angle of propagation θ_{kB}.

rium state. It makes no reference to the influence of the resulting distortions of the particle distribution functions on a long time-scale evolution. In particular, as the wave amplitude increases, quasi-linear effects may compete with other processes possibly acting in the opposite direction. In particular, when the wave frequencies are much smaller than the proton gyrofrequency, plasma heating can originate from the non-resonant action of low-frequency Alfvén waves.[24–26] In this regime, the stochastic heating resulting from particle acceleration due to electric field fluctuations at the scale of the ion Larmor radius breaks the conservation of the magnetic moment and leads to perpendicular heating.[27,28]

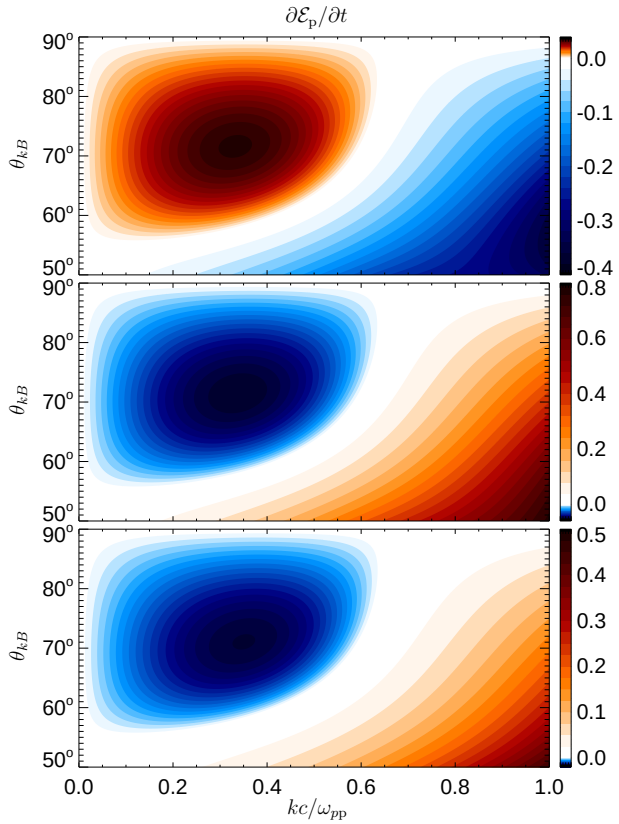

FIG. 8. Proton heating rates for mirror modes in the unstable regime: Color scale plots of the parallel (top), perpendicular (middle) and total (bottom) heating rates as functions of the wave vector k and the angle of propagation θ_{kB}. The corresponding color scales are shown at right (red shades indicate positive values, and blue shades negative ones).

This effect was however studied by considering particles propagating in the electromagnetic field associated with prescribed waves, neglecting any feedback of the particles on the waves.

APPENDIX: GLOSSARY

We use the following notations: t holds for the time, the subscript s refers to the different particle species (e: electrons, p: protons), i is the imaginary unit, $\Re$ and $\Im$ indicate the real and imaginary part, respectively. Overline indicates the complex conjugate, $\overline{a+ib} = a - ib$ for real a and b. Furthermore, ω is the complex frequency, with $\omega_r = \Re\omega$ and $\gamma = \Im\omega$.

We denote by $\boldsymbol{E}$ and $\boldsymbol{B}$ the electric and magnetic fields, while $\boldsymbol{B}_0$ is the ambient magnetic field and $B_0 = |\boldsymbol{B}_0|$ its magnitude. Here $f_s = f_s(v_\parallel, v_\perp)$ is the normalized velocity distribution function, with $v_\parallel$ and $v_\perp$ referring to the velocity components parallel and perpendicular to $\boldsymbol{B}_0$, respectively. Here $\delta\boldsymbol{E}$ and $\delta\boldsymbol{B}$ are the linear electric and magnetic field components of a given linear mode. The wave vector $\boldsymbol{k}$ has components $k_\parallel$ and $k_\perp$, parallel

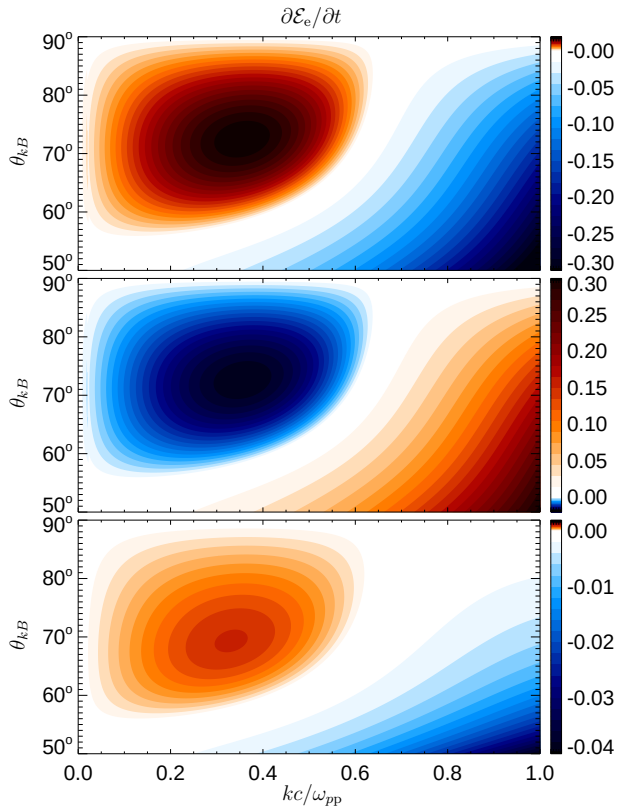

FIG. 9. Same as Fig. 8 for the parallel (top), perpendicular (middle) and total (bottom) electron heating rates due to mirror modes.

and perpendicular with respect to $\boldsymbol{B}_0$.

The cyclotron and plasma frequencies are denoted by $\omega_{cs} = q_s B_0/m_s$ and $\omega_{ps} = (n_s q_s^2/m_s\epsilon_0)^{1/2}$ respectively. In these expressions m_s, q_s, and n_s hold for the mass, the charge, and the number density, and ϵ_0 and μ_0 refer to the vacuum electric and magnetic permeability. Furthermore, $p_{s\parallel} = m_s n_s \int v_\parallel f_s \, \mathrm{d}^3v$ stands for the particle parallel linear momentum, $\mathcal{E}_{s\parallel} = m_s n_s \int f_s v_\parallel^2 \mathrm{d}^3v/2$, $\mathcal{E}_{s\perp} = m_s n_s \int f_s v_\parallel^2 \mathrm{d}^3v/2$ and $\mathcal{E}_s = \mathcal{E}_{s\parallel} + \mathcal{E}_{s\perp}$ for the parallel, perpendicular and total particle kinetic energies. Moreover, $\mathcal{E}_{em} = \epsilon_0|\delta\boldsymbol{E}|^2/2 + |\delta\boldsymbol{B}|^2/(2\mu_0)$ is the fluctuating electromagnetic energy of a given mode.

ACKNOWLEDGMENTS

The research leading to these results has received funding from the European Commission's Seventh Framework Programme (FP7) under the grant agreement SHOCK (project number 284515, project-shock.eu). This work was also supported by grants P209/12/2023 and P209/12/2041 of the Czech Science Foundation and by projects RVO:67985815 and RVO:68378289.

[1] T. H. Stix, *Waves in plasmas* (AIP, New York, 1992).
[2] A. A. Vedenov, E. P. Velikhov, and R. Z. Sagdeev, Nucl. Fusion **1**, 82 (1961).
[3] W. E. Drummond and D. Pines, Nucl. Fusion, Suppl. **3**, 1049 (1962).
[4] C. F. Kennel and F. Engelmann, Phys. Fluids **9**, 2377 (1966).
[5] S. P. Gary and R. L. Tokar, J. Geophys. Res. **90**, 65 (1985).
[6] P. Hellinger and P. M. Trávníček, J. Geophys. Res. **116**, A11101 (2011).
[7] V. D. Shapiro and V. I. Shevchenko, Sov. Phys. JETP, Engl. Transl. **18**, 1109 (1964).
[8] R. C. Davidson, D. A. Hammer, I. Haber, and C. E. Wagner, Phys. Fluids **15**, 317 (1972).
[9] R. C. Davidson and J. M. Ogden, Phys. Fluids **18**, 1045 (1975).
[10] P. H. Yoon, Phys. Fluids B **4**, 3627 (1992).
[11] A. Barnes, Phys. Fluids **11**, 2644 (1968).
[12] E. Marsch and C.-Y. Tu, J. Geophys. Res. **106**, 8357 (2001).
[13] P. Hellinger and P. M. Trávníček, Phys. Plasmas **19**, 062307 (2012).
[14] P. H. Yoon and J. Seough, **117**, A08102 (2012).
[15] M. L. Goldstein, H. K. Wong, and A. F. Viñas, J. Geophys. Res. **90**, 302 (1985).
[16] P. Hunana, M. L. Goldstein, T. Passot, P. L. Sulem, D. Laveder, and G. P. Zank, Astrophys. J. **766**, 93 (2013).
[17] S. P. Gary, *Theory of Space Plasma Microinstabilities* (Cambridge Univ. Press, New York, 1993).
[18] A. Hasegawa, Phys. Fluids **12**, 2642 (1969).
[19] P. Hellinger, Phys. Plasmas **14**, 082105 (2007).
[20] P. Hellinger, E. A. Kuznetsov, T. Passot, P. L. Sulem, and P. M. Trávníček, Geophys. Res. Lett. **36**, L06103 (2009).
[21] P. Hellinger, P. Trávníček, and J. D. Menietti, Geophys. Res. Lett. **31**, L10806 (2004).
[22] E. Quataert, Astrophys. J. **500**, 978 (1998).
[23] P. Hellinger, P. M. Trávníček, Š. Štverák, L. Matteini, and M. Velli, J. Geophys. Res. **118**, 1351 (2013).
[24] C. B. Wang, C. S. Wu, and P. H. Yoon, Phys. Rev. Lett. **96**, 125001 (2006).
[25] B. D. G. Chandran, B. Li, B. N. Rogers, E. Quataert, and K. Germaschewski, Astrophys. J. **720**, 503 (2010).
[26] Y. Nariyuki, T. Hada, and K. Tsubouchi, Phys. Plasmas **17**, 072301 (2010).
[27] C. S. Wu and P. H. Yoon, Phys. Rev. Lett. **99**, 075001 (2007).
[28] S. Bourouaine, E. Marsch, and C. Vocks, Astrophys. J. Lett. **684**, L119 (2008).